

## ARTICLE TYPE

# Dexterous Robotic Manipulation using Deep Reinforcement Learning and Knowledge Transfer for Complex Sparse Reward-based Tasks

Qiang Wang<sup>1</sup> | Francisco Roldan Sanchez<sup>2,3</sup> | Robert McCarthy<sup>1</sup> | David Cordova Bulens<sup>1</sup> | Kevin McGuinness<sup>2,3</sup> | Noel O'Connor<sup>2,3</sup> | Manuel Wüthrich<sup>4</sup> | Felix Widmaier<sup>5</sup> | Stefan Bauer<sup>6</sup> | Stephen J. Redmond<sup>1,3</sup>

<sup>1</sup>University College Dublin, Ireland

<sup>2</sup>Dublin City University, Ireland

<sup>3</sup>Insight SFI Research Centre for Data Analytics, Ireland

<sup>4</sup>Harvard University, USA

<sup>5</sup>MPI for Intelligent Systems, Tübingen, Germany

<sup>6</sup>KTH Stockholm, Sweden

## Correspondence

\*S.J. Redmond, UCD School of Electrical and Electronic Engineering, Belfield, Dublin 4, Ireland. Email: stephen.redmond@ucd.ie

## Abstract

This paper describes a deep reinforcement learning (DRL) approach that won Phase 1 of the Real Robot Challenge (RRC) 2021, and then extends this method to a more difficult manipulation task. The RRC consisted of using a TriFinger robot to manipulate a cube along a specified positional trajectory, but with no requirement for the cube to have any specific orientation. We used a relatively simple reward function, a combination of goal-based sparse reward and distance reward, in conjunction with Hindsight Experience Replay (HER) to guide the learning of the DRL agent (Deep Deterministic Policy Gradient (DDPG)). Our approach allowed our agents to acquire dexterous robotic manipulation strategies in simulation. These strategies were then applied to the real robot and outperformed all other competition submissions, including those using more traditional robotic control techniques, in the final evaluation stage of the RRC. Here we extend this method, by modifying the task of Phase 1 of the RRC to require the robot to maintain the cube in a particular orientation, while the cube is moved along the required positional trajectory. The requirement to also orient the cube makes the agent unable to learn the task through blind exploration due to increased problem complexity. To circumvent this issue, we make novel use of a *Knowledge Transfer* (KT) technique that allows the strategies learned by the agent in the original task (which was agnostic to cube orientation) to be transferred to this task (where orientation matters). KT allowed the agent to learn and perform the extended task in the simulator, which improved the average positional deviation from 0.134 m to 0.02 m, and average orientation deviation from 142° to 76° during evaluation. This KT concept shows good generalisation properties and could be applied to any actor-critic learning algorithm.

## KEYWORDS:

Robotic Manipulation, Deep Reinforcement Learning, Real Robot Challenge, Sim-to-Real Transfer, Transfer Reinforcement Learning

# 1 | INTRODUCTION

Dexterous robotic manipulation is essential in many industrial and domestic settings. Traditional robotic manipulation controllers often rely on solving inverse kinematic equations<sup>5</sup>. The goal of this approach is to find the robotic joint angle time course to move the end-effector of a robotic system (arm, gripper, fingers, etc.) to a desired pose<sup>8</sup>. Because the solution to this problem is not unique, motion primitives (i.e., a set of pre-computed movements that a robot can take in a given environment) are typically used<sup>9,10</sup>. These primitives can each have a defined cost, allowing the robot to avoid non-smooth or other undesirable transitions. However, these techniques have poor generalization ability and require complex control system structures. More precisely, they require significant bespoke tailoring for each novel manipulation task, leading to high implementation times and costs. Moreover, current state-of-the-art in traditional robotic control strategies generally struggle in unstructured tasks, which require high degrees of dexterity.

Reinforcement learning (RL), a data-driven learning approach in which models are trained by rewarding or punishing an agent that is acting in a particular environment. RL shows promise<sup>22</sup> to replace traditional robotic control approaches. The goal of this learning paradigm is to maximize the cumulative sum of scalar or vector reward signals received by the agent in response to the actions that it takes<sup>39</sup> so that it learns how to interact appropriately with the environment; that is, it learns how to act in order to maximize the rewards it can receive. However, traditional RL is unable to solve tasks with continuous action and state space, due to their high dimensionality. In other words, there are infinite combinations of states and actions in a continuous space, and therefore traditional RL algorithms cannot learn the required mappings between state, action, and reward for these problems. Hence, the field of deep reinforcement learning (DRL)<sup>37</sup> has emerged; a new discipline combining deep learning (DL)<sup>38</sup> and RL, which inherits the capacity to deal with high-dimensional continuous data from DL and decision-making ability from RL. DRL methods have been able to obtain outstanding results in robotic manipulation<sup>6,7</sup>.

However, the data inefficiency of DRL is a major barrier to its application in real-world robotics: real robot data collection is time-consuming and expensive. Much DRL research to-date has focused on improving these data-efficiency issues. Due to their generally improved sample complexity, off-policy DRL methods<sup>32,34</sup> are often preferred to on-policy methods<sup>35,11</sup>. Model-based DRL methods, which explicitly learn a model of the environment, have been used to further improve sample efficiency<sup>13,14,15</sup>, and have seen success in real robot settings<sup>16</sup>. Moreover, offline DRL techniques seek to leverage previously collected data to accelerate learning<sup>17</sup>, and are able to learn dexterous real-world skills such as opening a drawer<sup>18</sup>. Imitation learning methods provide the policy with expert demonstrations to learn from<sup>19,20</sup>, enabling success in real robot tasks, such as peg insertion<sup>21</sup>. Finally, simulation-to-real (sim-to-real) transfer methods train a policy quickly and cheaply in simulation before deploying it on the real robot, where learning is significantly slower, and have notably been used to solve a Rubik's cube with a robot hand<sup>22</sup>. To account for simulator modelling errors, and to improve the policies ability to generalize to the real robot, sim-to-real approaches often employ domain randomisation<sup>23,24</sup> or domain adaptation<sup>26,27</sup> techniques. Domain randomization, which has been particularly effective<sup>22</sup>, randomizes the physics parameters in simulation to learn a robust policy that can adapt to the partially unknown physics of the real system.

The costly nature of real-robot experimentation has limited research related to robotic dexterous manipulation. In light of these issues, the Real Robot Challenge (RRC)<sup>1</sup> aims to advance the state-of-the-art in robotic manipulation by providing participants with remote access to a TriFinger robotic platform (see Figure 1 (b))<sup>2</sup>, allowing for free and easy real-robot experimentation. To further support ease of experimentation, users are also provided with a simulation of this robotic system (see Figure 1 (a)). Full details can be found in the 'Protocol' section of the RRC website<sup>1</sup>.

This paper aims to extend the task of Phase 1 of the RRC 2021 to a more difficult task of moving a cube along a 3D positional trajectory while also maintaining a desired orientation. The task of Phase 1 of the RRC 2021 consisted in moving a cube along a defined trajectory. So here we increase the difficulty of this task by requiring the cube orientation to match a target orientation throughout the trajectory. We formulated both tasks as a pure RL problem. The movement-related skills of the robot are entirely learned in simulation, hence reducing human involvement compared to traditional real-world learning methods. We chose to use the Deep Deterministic Policy Gradient (DDPG) algorithm, as it was shown to have an excellent performance in handling robotic manipulation tasks with continuous action and observation spaces<sup>32</sup>. We used a reward function composed of goal-based sparse rewards in conjunction with Hindsight Experience Replay (HER)<sup>33</sup> to teach the control policy to move the cube to the desired  $xy$  coordinates (in the first task, controlling cube position) and then also orientation (in the extended task). Simultaneously, a dense distance-based reward is employed to teach the policy to lift the cube to the desired  $z$  coordinate. Finally, we use a novel concept

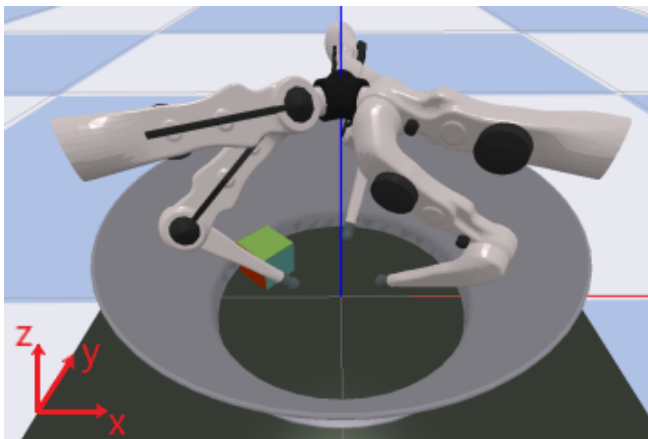
<sup>1</sup><https://real-robot-challenge.com>

that we call *knowledge transfer* (KT) facilitate learning during the task requiring cube position and orientation be controlled, which is based on the strategies previously-learned during the task requiring only the cube position be controlled. Compared with other methods used to solve a similar task<sup>4,35</sup>, our KT method has the advantage of being easier to implement, and can be extended to all actor-critic RL algorithms.

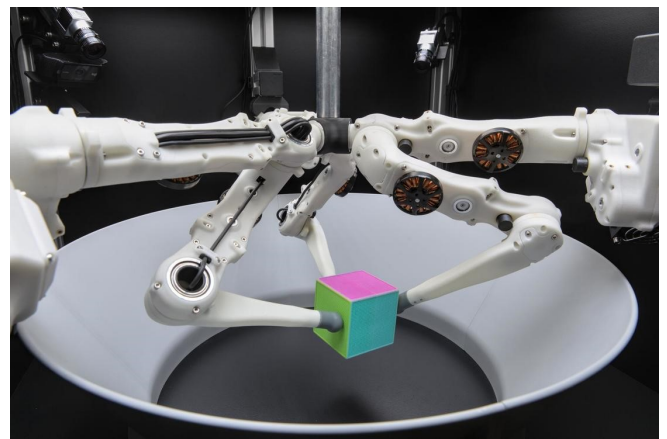
## 2 | METHODS

### 2.1 | Real Robot Challenge (RRC)

We were provided with remote access to well-maintained TriFinger robotic platforms<sup>2</sup> (see Figure 1 (b)) by the Max Planck Institute for Intelligent Systems (Tübingen/Stuttgart, Germany)<sup>2</sup>. To further support ease of experimentation, users are also provided with a simulated version of the robotic setup (see Figure 1 (a)). The 2021 RRC consists of an initial qualifying phase, performed purely in simulation, followed by independent Phases 1 and 2, both performed on the real robot. Full details can be found in the ‘Protocol’ section of the RRC website<sup>3</sup>.



(a) Visualisation of the PyBullet simulation environment for the TriFinger robot used in the RRC 2021.



(b) The real TriFinger robot used in the RRC 2021. Robot access to this system was possible, allowing competitors from around the world to test the policies learned in simulation the real robot. Competition results are generated from performance on this real-world system

**Figure 1** The TriFinger robot in: (a) the PyBullet<sup>30</sup> simulation, and; (b) the real world. Three identical robotic fingers are uniformly placed around the circular arena. The colored cube is the target object that must be moved.

#### 2.1.1 | Phase 1 task: Following a 3D position trajectory

Competition participants are tasked with solving the ‘*Move Cube on Trajectory*’ task. In this task, a cube must be carried along a goal trajectory, which specifies the Cartesian coordinates at which the cube should be positioned at each time-step<sup>4</sup>. The goals are sampled discretely, and the time interval between the two goals in the training phase can be defined manually. The robot should react as soon as the new goal is received obtain a higher score. For the final evaluation, multiple previously-unseen goal trajectories must be followed. Each evaluation trajectory consists of 120,000 time-steps, with 10 different coordinates that must be visited by the cube. The structure of the trajectory is such that the next goal (of 10 in total) is introduced at each of the following

<sup>2</sup><https://is.mpg.de/>

<sup>3</sup><https://real-robot-challenge.com>

<sup>4</sup>Agents interact with the environment in (discrete) time-steps, which are incremented after the agent takes an action

time-steps,  $t \in \{0, 30000, 40000, 50000, \dots, 110000\}$ . The obtained score,  $s_{pos}$  is defined by a distance-based weighted criterion:

$$s_{pos} = -\frac{1}{2} \left( \frac{\|g'_{xy} - g_{xy}\|}{2d_r} + \frac{\|g'_z - g_z\|}{d_h} \right) \quad (1)$$

where  $g'_{xy}$  and  $g'_z$  are the actual  $xy$  and  $z$  coordinates of the cube, respectively, and  $g_{xy}$  and  $g_z$  are the desired  $xy$  and  $z$  coordinates of the cube.  $d_r$  and  $d_h$  are constants representing the radius of the arena floor and the maximum height fingertips can reach. A higher score, averaged across all tested trajectories, implies a better manipulation performance.

Unlike end-to-end pick-and-place manipulation, the goals are continuously changing in this task. Various action strategies, such as pushing, cradling, or pinching, must be dynamically employed to move the cube in response to the changing positional goals.

### 2.1.2 | Extended task with increased difficulty: Position and orientation trajectory

We extended the task described above by introducing the an orientation trajectory goal in addition to the positional; this was inspired by the most challenging task in the RRC 2020<sup>5</sup>, where the cube must not only be moved to the desired position but also aligned with the desired orientation. The task in 2020 is a single end-to-end movement, rather than trajectory. Hence, we integrated position, orientation, and trajectory together to formed up a more challenging task that we named *Move Cube on Trajectory Pro*. To evaluate performance during this task we used the criterion used in RRC 2020 (c.f., Eq. (2))

$$s_{pos+ori} = -\left\| \left( R(g'_o) \right)^{-1} R(g_o) \right\| + s_{pos} \quad (2)$$

where the  $g'_o$  and  $g_o$  are the achieved orientation and the desired orientation, respectively, described using quaternions.  $R$  is the rotation matrix derived from the quaternions representation and  $^{-1}$  is the inverse matrix operator. Note,  $s_{pos}$  from Eq. (1) is incorporated in the calculation of  $s_{pos+ori}$  to evaluate the cube's position.

## 2.2 | Simulated environment

### 2.2.1 | Actions and observations

Pure torque control of the robot arms is employed with an update frequency of 20 Hz (i.e., each time-step in the environment is 0.05 seconds). The robot has three arms, with three motorized joints in each arm; thus, the action space is 9-dimensional (and continuous). Observations include: (i) robot joint positions, velocities, and torques; (ii) cube's current pose (i.e., its position and orientation, which in simulation is read directly from the simulator with no measurement error, and for the real world arena is estimated using provided computer vision object detection and segmentation methods), along with the difference between the poses at current and previous time-steps; and (iii) the current goal pose. In total, the observation space has 44 dimensions for the *Move Cube on Trajectory* task, and 48 for the *Move Cube on Trajectory Pro*.

In the *Move Cube on Trajectory* task, there are three target variables (three Cartesian position coordinates). In the *Move Cube on Trajectory Pro* task, there are seven target variables, representing 3D position and an additional four quaternion variables representing 3D orientation.

### 2.2.2 | Episodes

In each simulated training and testing episode, the robot begins in its default position. The simulator instantiates the cube and the arena environment, with the cube's initial position randomly sampled from the arena floor. Each episode lasts 90 time-steps, and the goal trajectory contains three desired goals, which are randomly sampled from the arena 3D space. The intervals between goals are same; i.e., the goal changes every 30 steps.

### 2.2.3 | Domain randomization

To help the learned policy generalize from a potentially inaccurate simulation to the real environment, we used some basic domain randomization (DR) techniques<sup>6</sup> (i.e., physics randomization). This includes uniformly sampling, from a specified range, parameters of the simulation physics (e.g., robot mass, restitution, damping, friction; see our code for more details<sup>7</sup>) and cube

<sup>5</sup><https://real-robot-challenge.com/2020>

<sup>6</sup>Our domain randomization implementation is based on the benchmark code from the 2020 RRC<sup>3</sup>.

<sup>7</sup>[https://github.com/RobertMcCarthy97/rrc\\_phase1](https://github.com/RobertMcCarthy97/rrc_phase1)

properties (mass and width) for each episode. To account for noisy real robot actuation and observations, uncorrelated noise is added to actions and observations during simulated episodes.

DR is only applied in the *Move Cube on Trajectory* task, since it requires sim-to-real transfer. In our final approach, we train the agent initially in the simulated non-DR environment for 300 epochs to allow it to learn the optimal policy quickly and easily. Afterward, the agent is tuned in the simulated DR environment for 100 epochs to enhance its robustness, before deploying to the real TriFinger robot.

## 2.3 | Learning algorithm

The goal-based nature of the *Move Cube on Trajectory* and *Move Cube on Trajectory Pro* tasks makes HER a good choice of learning algorithm; HER has excelled in similar goal-based robotic tasks<sup>33</sup> and obviates the need for complex reward engineering. As such, we combine DDPG and HER to make our RL algorithm<sup>8</sup>. However, in our early experiments we observed that the standard DDPG plus HER learning algorithm was slow in learning to lift the cube. To resolve this issue, we slightly altered the HER process and incorporated an additional dense reward which encourages cube-lifting behaviors. We describe this amendment below.

### 2.3.1 | Rewards and HER

In our approach, the reward function that guides the RL agent's learning consists of three components: (i) a sparse reward based on the cube's  $xy$  coordinates, termed  $r_{xy}$ ; (ii) a dense reward based on the cube's  $z$  coordinate, termed  $r_z$  (the coordinate frame can be seen in Figure 1 (a)); and (iii) a sparse reward based on the cube's 3D orientation (used in the *Move Cube on Trajectory Pro* task only).

The sparse  $xy$  reward,  $r_{xy}$ , is calculated as:

$$r_{xy} = \begin{cases} 0 & \text{if } \|g'_{xy} - g_{xy}\| \leq 2 \text{ cm} \\ -1 & \text{otherwise} \end{cases} \quad (3)$$

where  $g'_{xy}$  are the  $xy$  coordinates of the *achieved* goal (the actual  $xy$  coordinates of the cube), and  $g_{xy}$  are the  $xy$  coordinates of the *desired* goal.

The dense  $z$  coordinate reward,  $r_z$ , is defined as:

$$r_z = \begin{cases} -a \|z_{cube} - z_{goal}\| & \text{if } z_{cube} < z_{goal} \\ -\frac{a}{2} \|z_{cube} - z_{goal}\| & \text{if } z_{cube} > z_{goal} \end{cases} \quad (4)$$

where  $z_{cube}$  and  $z_{goal}$  are the  $z$  coordinates of the cube and goal, respectively, and  $a$  is a parameter which weights  $r_z$  relative to  $r_{xy}$ ; we use  $a = 20$ .

The sparse reward for the orientation is defined as:

$$r_{ori} = \begin{cases} 0 & \text{if } \|(R(g'_o))^{-1} R(g_o)\| \leq 0.384 \text{ rad (i.e., } 22^\circ) \\ -1 & \text{otherwise} \end{cases} \quad (5)$$

where the  $g'_o$  and  $g_o$  are the *achieved* orientation and the *desired* orientation represented as quaternions.  $R$  indicates rotation matrix calculation and  $^{-1}$  is the matrix inverse operator. We set the position (2 cm) and orientation ( $22^\circ$ ) thresholds as per Andrychowicz *et al.*<sup>12</sup>.

Another pure distance-based reward is also used as a comparator for our position-based reward scheme. This reward is popular in the field because of its clear geometric meaning and its computational efficiency:

$$r_{dis} = -\|g'_{xyz} - g_{xyz}\| \quad (6)$$

where  $g'_{xyz}$  and  $g_{xyz}$  are the *achieved*  $xyz$  coordinates and the *desired*  $xyz$  coordinates of the cube.

For the position-only *Move Cube on Trajectory* task, we only apply HER to the  $xy$  coordinates of the goal; i.e., the  $xy$  coordinates of the goal can be altered in hindsight, but the  $z$  coordinate remains unchanged. Thus, our HER altered goals are:

<sup>8</sup>Our DDPG + HER implementation is taken from <https://github.com/TianhongDai/hindsight-experience-replay>, and uses hyperparameters largely based on<sup>28</sup>.

$\hat{g} = (g'_{xy}, g_z)$ , meaning only  $r_{xy}$  is recalculated after HER is applied to a transition sampled during policy updates. This reward system is motivated by the following:

1. Using  $r_{xy}$  with HER allows the agent to learn to push the cube around in the early stages of training, even if it cannot yet lift the cube to reach the  $z$  coordinate of the goal. As the agent learns to push the cube around in the  $xy$  plane of the arena floor, it can then more easily stumble upon actions which lift it. Importantly, the approach of using  $r_{xy}$  with HER requires no bespoke reward engineering.
2.  $r_z$  aims to explicitly teach the agent to lift the cube by encouraging minimisation of the vertical distance between the cube and the goal. It is less punishing when the cube is above the goal, serving to further encourage lifting behaviours.
3. In the early stages of training, the cube mostly remains on the floor. During these stages, most  $g'$  sampled by HER will be on the floor. Thus, applying HER to  $r_z$  could often lead to the agent being punished for briefly lifting the cube. Since we only apply HER to the  $xy$  coordinates of the goal, our HER altered goals,  $\hat{g}$ , maintain their original  $z$  height. This leaves more room for the agent to be rewarded by  $r_z$  for any cube lifting it performs.

In the *Move Cube on Trajectory Pro* task, the reward of the positional components is same as above. HER is applied on the orientation and thus the HER altered goals are  $\hat{g} = (g'_{xy}, g'_{ori}, g_z)$ . Finally all items are summed to form the final reward,  $r = r_{xy} + r_z + r_{ori}$

### 2.3.2 | Goal trajectories

In each episode, the agent is faced with multiple goals; it must move the cube from one goal to the next along a given trajectory. To ensure the HER process remains meaningful in these multi-goal episodes, we only sample future achieved goals,  $g'$ , (to replace  $g$ ) from the period of time in which  $g$  was active.

In our implementation, the agent is unaware that it is dealing with trajectories: when updating the policy with transitions  $(s_t, g_t, a_t, r_t, s_{t+1}, g_{t+1})$  we always set  $g_{t+1} = g_t$ , even if in reality  $g_{t+1}$  was different<sup>9</sup>. Thus, the policy focuses solely on achieving the current active goal and is unconcerned with any future changes in the active goal.

### 2.3.3 | Exploration vs exploitation

We derive our DDPG-HER hyperparameters from Plappert *et al.*<sup>28</sup>, who use a highly exploratory policy when collecting data in the environment: with probability 30% a random action is sampled (uniformly) from the action-space, and when policy actions are chosen, Gaussian noise is applied. This is beneficial for exploration in the early stages of training, however, it can be limiting in the later stages when the policy must be fine-tuned; we found that the exploratory policy repeatedly drops the cube due to the randomly sampled actions and the injected action noise. To resolve this issue, rather than slowly reducing the level of exploration each epoch (which would require a degree of hyperparameter tuning), we make efficient use of evaluation episodes (which are performed by the standard exploitation policy) by adding them to the replay buffer. Thus, 90% of rollouts added to the buffer are collected with the exploratory policy, and the remaining 10% with the exploitation policy. This addition was sufficient to boost final success rates in simulation from 70-80% to >90% (where "success rate" is equivalent to that seen in Figure 2 ).

## 2.4 | Knowledge transfer

The signal from our computationally simple reward rarely guides the agent to focus on playing with the cube in the early training stage; hence, the agent's learning relies heavily on pure exploration. However, its arbitrary exploration is unlikely to explore actions that change the cube's orientation. Unlike the position-only *Move Cube on Trajectory* task, the orientation exploration in the *Move Cube on Trajectory Pro* task is comparatively more difficult, requiring the cube to be both lifted and rotated simultaneously. To this end, we introduce our KT approach, which transfers a trained agent's knowledge (*teacher*) to another untrained agent (*student*), or uses the *teacher*'s knowledge to assist the *student* with learning. In our case, we train a *teacher* from the position-only *Move Cube on Trajectory* task, and train *students* in the *Move Cube on Trajectory Pro* task. The *teacher*'s transferred knowledge increases the likelihood of the *student* discovering useful actions to control the orientation of the

<sup>9</sup>Interestingly, we found that exposing the agent (during updates) to transitions in which  $g_{t+1} \neq g_t$  hurt performance significantly, perhaps due to the extra uncertainty this introduces to the DDPG action-value estimates.

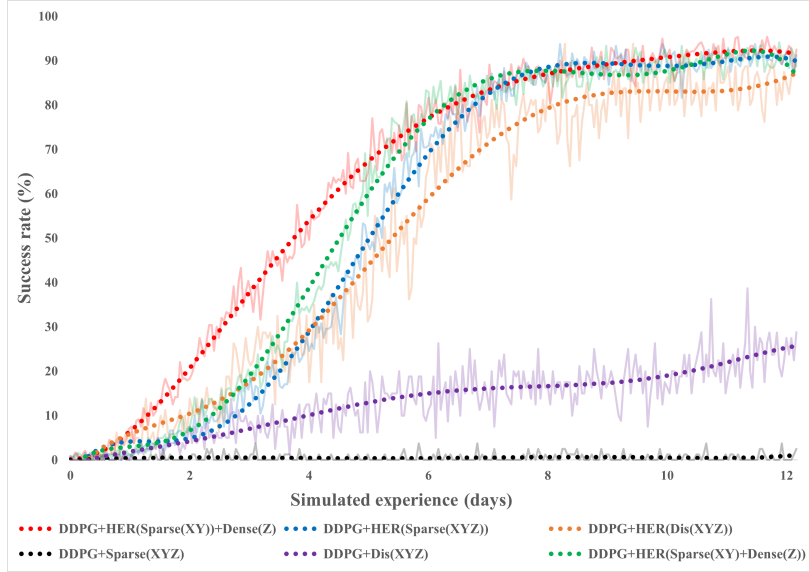


**Figure 2** Success rate vs experience collected during simulated training (1 day in simulator,  $\approx 1.7$  million environment steps). We took the average over 3 randomly-selected seeds for this illustration. The solid dotted lines are the trend lines and the faded lines are the raw data. An episode is deemed successful if, when complete, the final goal of the trajectory has been achieved. We compare training with: (i) Our final method where HER is applied to  $r_{xy}$  but not to  $r_z$  (red); (ii) HER applied to both  $r_{xy}$  and  $r_z$  (green); (iii) HER applied to a standard sparse reward where  $xyz$  are calculated together (blue); (iv) HER applied to pure distance reward,  $r_{dis}$ , where  $xyz$  are calculated together (orange); and (v) Pure distance reward,  $r_{dis}$ , without HER (purple); (vi) Standard sparse reward without HER (black).

cube through exploring in the early stages of training, instead of exploring all possible actions at random, as the *student* has been transferred the knowledge required to control the cube’s position; in this way, we expect the agent to learn how to control the cube’s orientation more quickly. We use two strategies ensure the *teacher’s* guidance not too biased toward position-based exploration: 1) increasing the action noise in the early stages of exploration; 2) choose a *teacher* that has weaker performance in the *Move Cube on Trajectory* task (i.e., success rate of only 80%).

We have the following three implementations of KT. We name them differently for ease of explanation later.

1. **ACTOR-CRITIC**: Initialise the *student’s* actor and critic<sup>10</sup> network weights by loading the *teacher’s* trained weights.
2. **ACTOR**: Initialise the *student’s* actor network weights by loading the *teacher’s* trained weights and randomly initialize the *student’s* critic.
3. **COLLECT**: The *student* does not inherit any network weights from the *teacher*. The *teacher* only helps the *student* to collect experience in the early stages of training. Both the student’s actor and critic networks are randomly initialized. As the *teacher’s* knowledge is not updated in the new task, the collected experience lacks diversity. Hence, we force the *teacher’s* participation to decay as training progresses, allowing the *students* to engage in exploration further, making the experience more beneficial to the *student*.
4. **SCRATCH**: The attempt to solve the *Move Cube on Trajectory Pro* task, ‘from scratch’, without using KT. This is used for comparing with KT approaches.

## 2.5 | Train, test, and evaluate

All training and testing were performed on the Sonic high performance cluster at University College Dublin, Ireland. For our training, jobs are randomly assigned to Dell machines configured with R640 2x Intel Xeon Gold 6152 (2.1 GHz, 22 cores) or

<sup>10</sup>The *actor* is typically a policy function, which outputs actions to interacts with the environment. The *critic* uses approximate architecture and simulations to learn a value function, which is then used to update the *actors’* policy parameters<sup>40</sup>.

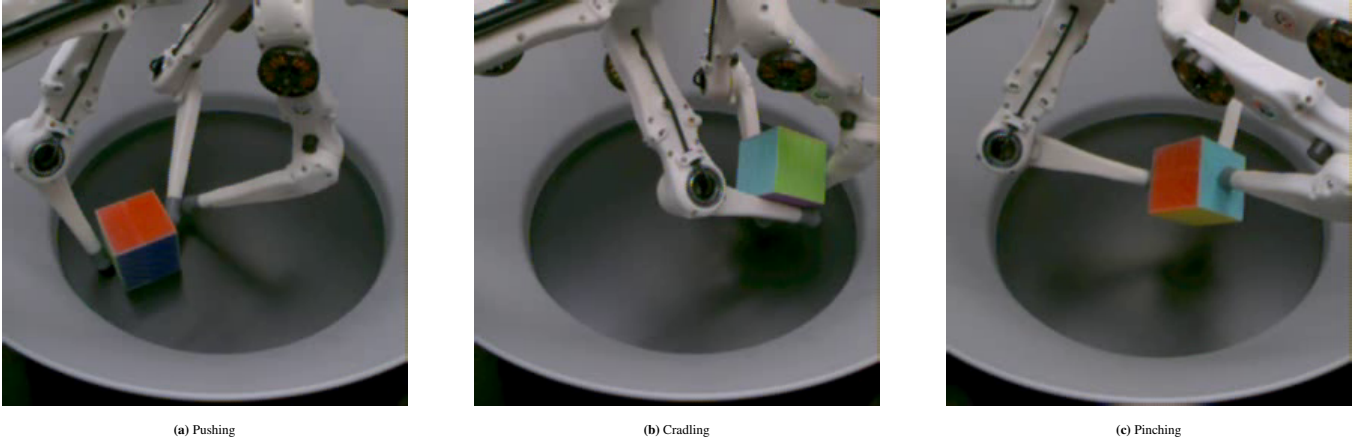


**Figure 3** The various manipulation strategies learned by the agent: (a) pushing; (b) cradling; (c) pinching.

C6200 V2 2x Intel E5-2660 v2 (2.2 GHz, 10 cores). In each training run, eight RL agents are assigned to eight processors and run in parallel. At the end of each training step, the neural network weights of 8 agents are synchronized by averaging. The experiences collected by agents are stored in their respective experience replay buffers and will not be shared. The global success rate and reward are calculated by averaging the local values from eight agents.

- **Training:** For the *Move Cube on Trajectory* task, each job runs for 300 epochs, overall interacting with the simulated environment for 21.6 million time-steps (2.7 million time-steps for each RL agent). The neural network of each agent is updated 15,000 times and synchronization is performed after each update. For the *Move Cube on Trajectory Pro* task, the number of training epochs is increased to 500, and other training parameters increased proportionally.
- **Testing:** Testing is performed after each training epoch. Each agent runs for 900 time-steps in the simulator. Experience collected from testing is stored in the replay buffer. The neural network losses, success rates and rewards of eight agents are averaged and saved.
- **Real robot evaluation of Move cube on Trajectory:** For the *Move cube in trajectory* task performed on the real TriFinger robot, we adopt the evaluation criteria set by the RRC 2021. For each evaluation episode, a random goal trajectory is sampled. Each test run keeps 120,000 time-steps, with 10 different goals (first goal at first time-step, then 30,000 time-steps to the second goal, and 10,000 time-steps for each of the remaining 8 goals after that). The domain gap between simulation and reality was significant, and generally led to inferior scores on the real robot. Policies often struggled to gain control of the real cube which appeared to slip more easily from the fingers than in simulation. Additionally, on the real robot, policies could become stuck with a fingertip pressing the cube into the wall. As a makeshift solution to this issue, we assumed the policy was stuck whenever the cube had not reached the goal's  $x,y$  coordinates for 50 consecutive steps; then uniformly sampled random actions were taken for 7 time-steps in an attempt to free the policy from its stuck state.

### 3 | RESULTS

#### 3.1 | RRC 2021 Phase 1

##### 3.1.1 | Learning outcomes of RL agents

Our method is highly effective in simulation. The algorithm can learn from scratch to proficiently grasp the cube and lift it along goal trajectories. Figure 2 compares the training performance of our final algorithm (red curve) to that of other combinations<sup>11</sup>. Our algorithm appears to converge stably and more quickly than either HER applied to a standard sparse reward or HER applied to both  $r_{xy}$  and  $r_z$ . Furthermore, HER plays a crucial role in the success of our algorithm. The pure DDPG agent finds it difficult

<sup>11</sup>These runs did not use domain randomization. Generally we trained from scratch in standard simulation before fine-tuning in a domain-randomized simulation



**Table 1** Self-reported (i.e., not reported by competition organizers) evaluation scores of our learned *pushing*, *cradling*, and *pinching* policies when deployed on the simulated and real robots (mean  $\pm$  standard deviation (SD) score over 10 episodes). Scores are based on the cumulative position error of the cube during an episode:  $s_{pos} = -\frac{1}{2} \sum_{t=0}^n \left( \frac{\|e_{xy}^t\|}{d_r} + \frac{|e_z^t|}{d_h} \right)$ , where  $e^t = (e_x^t, e_y^t, e_z^t)$  is the error between the cube and goal position at time-step  $t$ ,  $d_r$  the arena floor radius, and  $d_h$  the range on the z-axis.

	Pushing			Cradling			Pinching		
Simulation	-20,399	$\pm$	3,799	-6,349	$\pm$	1,039	<b>-6,198</b>	$\pm$	1,840
Real robot	-22,137	$\pm$	3,671	-14,207	$\pm$	2,160	<b>-11,489</b>	$\pm$	3,790

**Table 2** Evaluated score of RL agents trained under different random seeds; three seeds selected here for illustration. The RRC organizing institute has a small number of real robots available for remote use, with a small but expected variation the physical parameters of each arena and the performance of each robots. The evaluations are performed on three of these robots, chosen at random, named Roboch1, Roboch5 and Roboch6, to increase the generalizability of the results. Each evaluation is repeated 15 times (15 goal trajectories) with 120,000 time-steps in each repeat. The results from the simulator is also shows in the Sim subcolumns.

	Seed 0				Seed 123				Seed 200			
Robot (Real/Sim)	Robch1	Robch5	Robch6	Sim	Robch1	Robch5	Robch6	Sim	Robch1	Robch5	Robch6	Sim
Reward	-12175	-11300	-9913	<b>-5447</b>	-9308	-8926	-10017	<b>-6376</b>	-16266	-13120	-15750	<b>-7277</b>
Avg	<b>-11129</b>				<b>-9417</b>				<b>-15045</b>			

to learn from sparse rewards without HER, and the convergence speed is extremely slow for an agent guided by this traditional distance-based reward.

Throughout different training runs, our policies learned several different manipulation strategies, the most distinct of which included: ‘*pushing*’ the cube on the arena floor; (ii) ‘*cradling*’ the cube with all three of its forearms (not fingertips); and (iii) ‘*pinching*’ the cube with two fingertips and supporting it with the third (see Figure 3 ).

Our final policies transferred to the real robot with reasonable success. Table 1 displays the self-reported scores of our best *pinching* and *cradling* policies under RRC Phase 1 evaluation conditions. As a baseline comparison, we trained a simple ‘*pushing*’ policy which ignores the height component of the goal and simply learns to push the cube along the floor to the goal’s  $xy$  coordinates. The *pinching* policy performed best on the real robot, and is capable of carrying the cube along goal trajectories for extended periods of time, and of recovering the cube when it is dropped. This policy was submitted for the official RRC Phase 1 final evaluation round and obtained the winning score<sup>31</sup> (see <https://real-robot-challenge.com/leaderboard>, username ‘thriftysnipe’).

### 3.1.2 | Agents trained from different random seeds behave differently

We verified that discrepancies exist between agents’ performances when trained from different random seeds (see Table 2 )<sup>41</sup>. In our case, the random seed is used to randomly reset the environment and randomize actions so that agents can explore in the training phase. Interestingly, the best performing agent (Seed 0 in Table 2 ) in the simulator had a relatively poor performance on the real robot. This agent overfits to the simulator environment, and hence the acquired policy has low generalization capability. The agent train under (random) Seed 200 (see Table 2 ) did not obtain the optimal policy and performed the worst on the real robot.

### 3.1.3 | Domain randomization improves real robot performance

The performance of agents on the real robot significantly improved after tuning using DR (see Table 3 ). Among these agents, the agent trained from Seed 123 achieved simulator-level performance. Nonetheless, using DR from the beginning of training is not recommended (at least for our algorithm). In a domain-randomized simulation environment, the agent will be hindered in learning the optimal policy, compared to the policy learned in the standard simulation environment that does not use domain randomization (see Figure 4 ), and hence will achieve poor performance on the real robots (see Table 3 ). A demonstration video of this trained network in action can be seen in <https://www.youtube.com/watch?v=0Lpod542T9k>

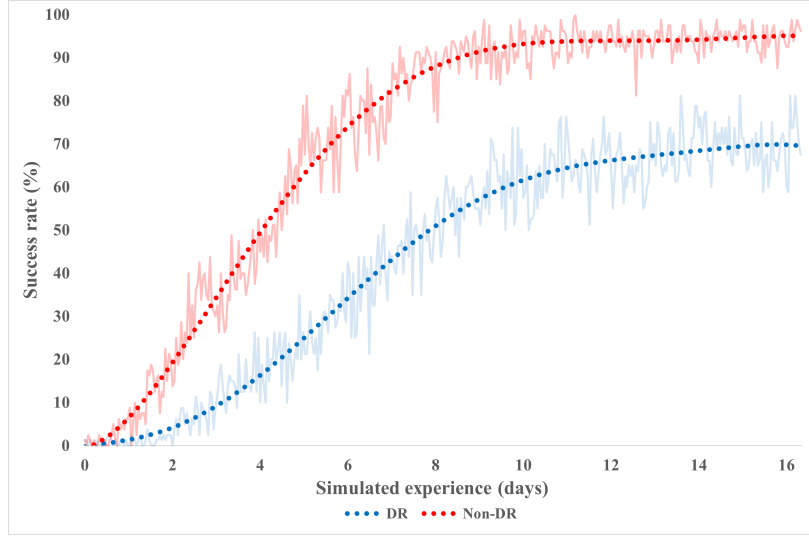


**Figure 4** Comparison between agents trained from scratch with domain randomization (DR) and without.

**Table 3** Evaluation rewards of different agents evaluated in simulation and on real robots; three seeds chosen at random to illustrate typical performance. Scratch(DR) represents the agent trained from scratch using DR from the beginning of training. Scratch(NDR) is the agent trained from scratch without using DR; Scratch(NDR) + Tune(DR) is the agent firstly trained from scratch without DR and then subsequently tuned using DR in a second training phase.

Seed	Type	Simulation	Real robot
0	Scratch(DR)	-8808	-16685
	Scratch(NDR)	-5447	-11129
	<b>Scratch(NDR) + Tune(DR)</b>	-5825	-8922
123	Scratch(DR)	-9873	-15726
	Scratch(NDR)	-6376	-9417
	<b>Scratch(NDR) + Tune(DR)</b>	-6253	-7030
200	Scratch(DR)	-11779	-15398
	Scratch(NDR)	-7277	-15045
	<b>Scratch(NDR) + Tune(DR)</b>	-6147	-8535

### 3.2 | Move Cube on Trajectory Pro

Figure 5 compares the training performance of different approaches to learning the *Move Cube on Trajectory Pro* task, including using our proposed KT scheme compared to not using it. Agents' overall rewards are decomposed into position and orientation components so that the learning outcomes of the two components can be compared.

Training using the combined DDPG and HER algorithm (not using KT, see *SCRATCH* curve in Figure 5) completely fails in the *Move Cube on Trajectory Pro* task, with rewards on all components staying at their minimum possible values. In contrast, agents in all three KT methods shows learning trends. Among them, both *COLLECT* and the *SCRATCH* use randomly initialized neural networks. However, with the help of the experience collected by the teacher, *COLLECT* shows a more successful learning performance.

By transferring the teacher's knowledge of how to perform the position-only task to the *ACTOR-CRITIC student*, the *ACTOR-CRITIC* excels in its ability to reach position targets from the beginning of training. This makes it more likely that the *ACTOR-CRITIC* will discover actions which change the cube's orientation and are rewarded. All agents learn orientation from scratch, while the *ACTOR-CRITIC* has a better learning performance than that of *COLLECT*. However, the *COLLECT* agent relies strongly on the experience collected by the *teacher* in the early stages of training, although we set a decay on the *teacher's* participation over time. Although the *ACTOR* agent inherits the knowledge of the *teacher's* actor, it performs the worst among all

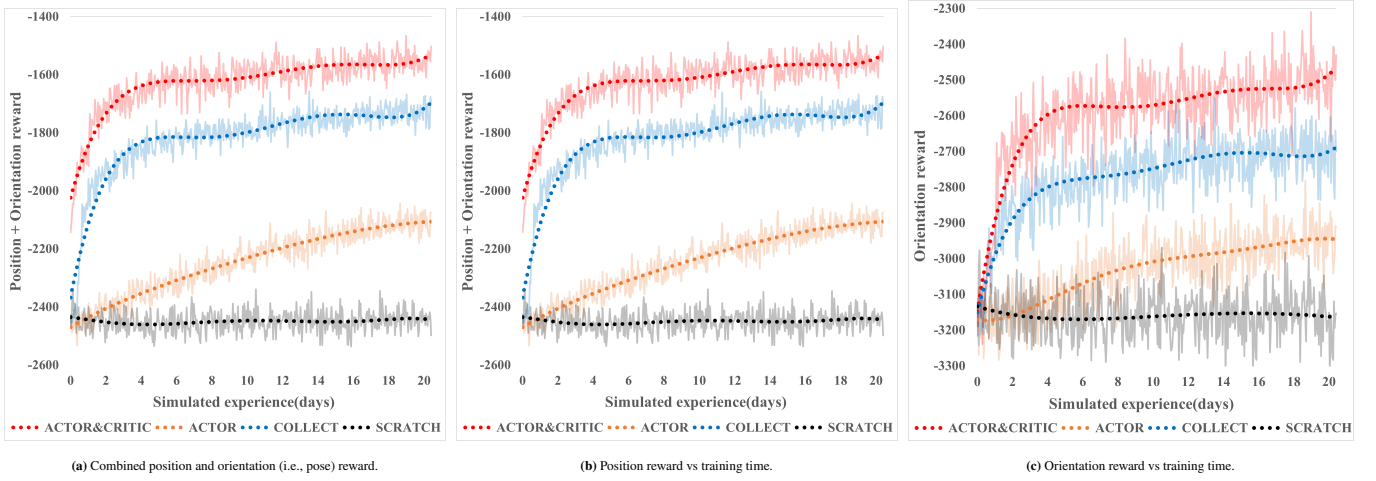


**Figure 5** Learning curves showing rewards achieved by agents using different learning algorithms.

**Table 4** The average deviations between achieved and desired position/orientation over 15 evaluation episodes in the simulator; each episode lasts 120,000 time-steps. The deviations are self-customized to see the learning outcomes intuitively. For the position:  $\mathbf{dev}_{\text{dis}} = ||g'_{xyz} - g_{xyz}||$ , which can measure the distance between the actual position of the cube and the goal position. For the orientation:  $\mathbf{dev}_{\text{angle}} = ||(R(g'_o))^{-1}R(g_o)||$ , which can measure the angle difference between the actual and target orientations. The deviations of all time-steps are accumulated and finally averaged.

	ACTOR-CRITIC	ACTOR	COLLECT	SCRATCH	TEACHER
Average position deviation (m)	<b>0.023</b>	0.066	0.031	0.134	0.024
Average orientation deviation (°)	<b>75.8</b>	98.6	84.9	142.2	126.2

KT strategies. Because the randomly-initialized critic is not compatible with the well-trained actor, and the critic's feedback cannot meet the actor's expectations; hence, the actor's performance worsens.

The evaluation results are shown in Table 4. All three methods enable the student agent to learn the *Move Cube on Trajectory Pro* task, but behave differently. Among them, the *ACTOR-CRITIC* agent can achieve comparable performance to the *teacher* at reaching position targets, and learn to perform very well on reaching orientation targets. A demonstration video of this trained network in action can be seen here: <https://www.youtube.com/watch?v=GhkCqoMqxU4>.

## 4 | CONCLUSION

Our relatively simple reinforcement learning approach fully solves the '*Move Cube on Trajectory*' task in simulation. Unlike the RRC 2020 benchmark solution<sup>3</sup>, this was achieved with the use of minimal domain-specific knowledge. We have only tried our approach using the DDPG learning algorithm; other later published DRL algorithms, such as SAC<sup>34</sup> or TD3<sup>36</sup> may have superior performance, and will be the focus of our future research.

Reproducing our method is highly feasible, since only one machine with eight processors is required; no GPUs are required. The number of agents can be set to more if an increase in training speed is possible. Or, the number of agents can be set to less, but sacrificing training speed.

Although our results in simulation were very good, the algorithm is somewhat sample inefficient, taking roughly 10 million environment steps to converge (equivalent to 6 days of simulated experience). Thus, another important direction for future work would be to increase sample efficiency; perhaps achievable via a model-based reinforcement learning approach<sup>14,29</sup>.

The reward function is the driver of DRL; a well-designed and well-shaped reward can improve the quality and speed of DRL<sup>4</sup>. A bespoke reward function might limit the utility of a method to a small range of tasks, and is likely costly to develop.

In contrast, goal-based sparse rewards can be easily created. Compared to shaped rewards, goal-based sparse rewards have an extremely weak reward signal. The agent can only get the bonus when succeeding in the task; otherwise, it gets punished. However, the probability of success in some tasks is very low, and a dearth of positive feedback hinders improvement in the task. HER can effectively enhance sparse reward signals by modifying the experience data before giving it to the agent. Typically, HER replaces the goal with the posterior state, making the prior-posterior transition highly likely to succeed by the action applied to the prior state. HER has been proved to work wonders<sup>33</sup> in sparse-reward-based tasks, as verified in our case.

In addition, our distance-based dense reward can effectively accelerate the agent’s learning in the early stages of training, and its implementation is straightforward. It can be easily extended to other robotic manipulation tasks.

Moreover, our learned policies can successfully implement their sophisticated manipulation strategies on the real robot through our DR tuning approach, which bridges the large sim-to-real domain gap and allows the achievement of near-simulator-level performance on real robots. In the RRC 2021, which used the *Move Cube on Trajectory* task, requiring only position targets be reached, we outperformed all competing submissions, including those employing more classical robotic control techniques. The sim-to-real transfer is an essential means to bring robotic learning into reality. Training an intelligent robotic controller in the real world is expensive and impractical. Take an example of a problem we faced before: we tried to collect the data from the real TriFinger robots to train an agent from scratch; however, a large number of interactions caused a lot of friction between the finger and the cube, resulting in wear and tear, which adhered to the surface of the cube and interfered with the estimation of the cube’s pose by machine vision algorithms. Indeed, the main limitation of our approach was the absence of any real-robot data. It is likely that some fine-tuning of the policy on real data would greatly increase its robustness in the real environment, and developing a technique which could do so efficiently is one direction for future work.

There is some variance between agents trained under different seeds. Some agents perform excellently in the simulator while having poor performance on real robots, as they overfit the simulated environment. In contrast, some agents cannot acquire the optimal strategies in the simulator, even if using the same algorithm, and ultimately perform poorly on the real robot. Hence, when applying the DRL controller on a real robot through sim-to-real transfer, do not easily trust the agent that performs best in the simulator. It is wise to try multiple trained agents on the real robot and select the best.

Our novel KT approach can enable an agent to perform more useful interactions with the environment in the early stages of learning, helping to avoid exploration actions that do not result in learning experiences. It allows the complex *Move Cube on Trajectory Pro* task to be solved efficiently in the simulator. Additionally, KT increases resource utilization efficiency, avoiding repeatedly re-learning similar skills. It may be feasible to deploy this method in any actor-critic RL algorithm, and the implementation method is straightforward. A future similar, but innovative research direction would be to train a master *teacher* with broad knowledge in complex environments and use it widely in various downstream tasks<sup>25</sup>.

The development of DRL-driven robotic manipulation is still an unsolved problem, but is currently receive a lot of attention from the research community. Solving this problem will have a huge impact on industry and society in general. At present, the training of DRL agents is mostly carried out in the simulator, using perfect feedback data which is mostly vision-based. The current capabilities of simulators to render realistic mechanics, including the friction, texture, and deformations at contact interfaces between robotic fingers and the objects they manipulate, are very basic. However, as such simulations improve, and the ability of real world robots to sense these same contact mechanics advances in tandem, we can expect significant improvements in the dexterity of DRL-based robotic manipulation systems. Through this ability to dexterously interact with and learn from the world is surely the path to developing systems with superior intelligence.

## ACKNOWLEDGMENTS

This publication was supported by a Science Foundation Ireland President of Ireland Future Research Leaders Award (17/FRL/4832), by the Insight SFI Research Centre for Data Analytics (SFI/12/RC/2289\_P2) co-funded by the European Regional Development Fund, and by the China Scholarship Council (CSC). We acknowledge the Research IT HPC Service at University College Dublin for providing computational facilities and support that contributed to the research results reported in this paper.

## References

1. Bauer, S., Widmaier, F., Wüthrich, M., Funk, N., De Jesus, J.U., Peters, J., Watson, J., Chen, C., Srinivasan, K., Zhang, J. and Zhang, J., 2021. A Robot Cluster for Reproducible Research in Dexterous Manipulation. arXiv preprint arXiv:2109.10957.

2. Wüthrich, M., Widmaier, F., Grimminger, F., Akpo, J., Joshi, S., Agrawal, V., Hammoud, B., Khadiv, M., Bogdanovic, M., Berenz, V. and Viereck, J., 2020. Trifinger: An open-source robot for learning dexterity. arXiv preprint arXiv:2008.03596.
3. Funk, N., Schaff, C., Madan, R., Yoneda, T., De Jesus, J.U., Watson, J., Gordon, E.K., Widmaier, F., Bauer, S., Srinivasa, S.S. and Bhattacharjee, T., 2021. Benchmarking structured policies and policy optimization for real-world dexterous object manipulation. *IEEE Robotics and Automation Letters*, 7(1), pp.478-485.
4. Allshire, A., Mittal, M., Lodaya, V., Makovychuk, V., Makoviichuk, D., Widmaier, F., Wüthrich, M., Bauer, S., Handa, A. and Garg, A., 2021. Transferring dexterous manipulation from gpu simulation to a remote real-world trifinger. arXiv preprint arXiv:2108.09779.
5. Liu, R., Nageotte, F., Zanne, P., de Mathelin, M. and Dresch-Langley, B., 2021. Deep reinforcement learning for the control of robotic manipulation: a focussed mini-review. *Robotics*, 10(1), p.22.
6. Nguyen, H. and La, H., 2019, February. Review of deep reinforcement learning for robot manipulation. In 2019 Third IEEE International Conference on Robotic Computing (IRC) (pp. 590-595). IEEE.
7. Kober, J., Bagnell, J.A. and Peters, J., 2013. Reinforcement learning in robotics: A survey. *The International Journal of Robotics Research*, 32(11), pp.1238-1274.
8. Wei, Hui, Yijie Bu, and Ziyao Zhu. "Robotic arm controlling based on a spiking neural circuit and synaptic plasticity." *Biomedical Signal Processing and Control* 55 (2020): 101640.
9. Cohen, Benjamin J., Sachin Chitta, and Maxim Likhachev. "Search-based planning for manipulation with motion primitives." 2010 IEEE International Conference on Robotics and Automation. IEEE, 2010.
10. Stulp, F., Theodorou, E., Kalakrishnan, M., Pastor, P., Righetti, L. and Schaal, S., 2011, September. Learning motion primitive goals for robust manipulation. In 2011 IEEE/RSJ International Conference on Intelligent Robots and Systems (pp. 325-331). IEEE.
11. Schulman, J., Levine, S., Abbeel, P., Jordan, M. and Moritz, P., 2015, June. Trust region policy optimization. In International conference on machine learning (pp. 1889-1897). PMLR.
12. Andrychowicz, O.M., Baker, B., Chociej, M., Jozefowicz, R., McGrew, B., Pachocki, J., Petron, A., Plappert, M., Powell, G., Ray, A. and Schneider, J., 2020. Learning dexterous in-hand manipulation. *The International Journal of Robotics Research*, 39(1), pp.3-20.
13. Deisenroth, Marc, and Carl E. Rasmussen. "PILCO: A model-based and data-efficient approach to policy search." *Proceedings of the 28th International Conference on machine learning (ICML-11)*. 2011.
14. Janner, M., Fu, J., Zhang, M. and Levine, S., 2019. When to trust your model: Model-based policy optimization. *Advances in Neural Information Processing Systems*, 32.
15. Hafner, D., Lillicrap, T., Ba, J. and Norouzi, M., 2019. Dream to control: Learning behaviors by latent imagination. arXiv preprint arXiv:1912.01603.
16. Nagabandi, A., Konolige, K., Levine, S. and Kumar, V., 2020, May. Deep dynamics models for learning dexterous manipulation. In *Conference on Robot Learning* (pp. 1101-1112). PMLR.
17. Levine, S., Kumar, A., Tucker, G. and Fu, J., 2020. Offline reinforcement learning: Tutorial, review, and perspectives on open problems. arXiv preprint arXiv:2005.01643.
18. Nair, A., Dalal, M., Gupta, A. and Levine, S., 2020. Accelerating online reinforcement learning with offline datasets. arXiv preprint arXiv:2006.09359.
19. Pastor, P., Hoffmann, H., Asfour, T. and Schaal, S., 2009, May. Learning and generalization of motor skills by learning from demonstration. In 2009 IEEE International Conference on Robotics and Automation (pp. 763-768). IEEE.
20. Johns, Edward. "Coarse-to-Fine Imitation Learning: Robot Manipulation from a Single Demonstration." arXiv preprint arXiv:2105.06411 (2021).
21. Vecerik, M., Hester, T., Scholz, J., Wang, F., Pietquin, O., Piot, B., Heess, N., Rothörl, T., Lampe, T. and Riedmiller, M., 2017. Leveraging demonstrations for deep reinforcement learning on robotics problems with sparse rewards. arXiv preprint arXiv:1707.08817.
22. Akkaya, I., Andrychowicz, M., Chociej, M., Litwin, M., McGrew, B., Petron, A., Paino, A., Plappert, M., Powell, G., Ribas, R. and Schneider, J., 2019. Solving rubik's cube with a robot hand. arXiv preprint arXiv:1910.07113.
23. Peng, X.B., Andrychowicz, M., Zaremba, W. and Abbeel, P., 2018, May. Sim-to-real transfer of robotic control with dynamics randomization. In 2018 IEEE international conference on robotics and automation (ICRA) (pp. 3803-3810). IEEE.
24. Tobin, J., Fong, R., Ray, A., Schneider, J., Zaremba, W. and Abbeel, P., 2017, September. Domain randomization for transferring deep neural networks from simulation to the real world. In 2017 IEEE/RSJ international conference on intelligent

- robots and systems (IROS) (pp. 23-30). IEEE.
25. XueBin Peng, Yunrong Guo, Lina Halper, Sergey Levine, Sanja Fidler. "Coarse-to-Fine Imitation Learning: Robot Manipulation from a Single Demonstration." arXiv preprint arXiv:2105.06411 (2021).
  26. Arndt, K., Hazara, M., Ghadirzadeh, A. and Kyrki, V., 2020, May. Meta reinforcement learning for sim-to-real domain adaptation. In 2020 IEEE International Conference on Robotics and Automation (ICRA) (pp. 2725-2731). IEEE.
  27. Eysenbach, B., Asawa, S., Chaudhari, S., Levine, S. and Salakhutdinov, R., 2020. Off-dynamics reinforcement learning: Training for transfer with domain classifiers. arXiv preprint arXiv:2006.13916.
  28. Plappert, M., Andrychowicz, M., Ray, A., McGrew, B., Baker, B., Powell, G., Schneider, J., Tobin, J., Chociej, M., Welinder, P. and Kumar, V., 2018. Multi-goal reinforcement learning: Challenging robotics environments and request for research. arXiv preprint arXiv:1802.09464.
  29. McCarthy, Robert, and Stephen J. Redmond. "Imaginary Hindsight Experience Replay: Curious Model-based Learning for Sparse Reward Tasks." arXiv preprint arXiv:2110.02414 (2021).
  30. Coumans, E., and Bai, Y., 2016 - 2021. PyBullet, a Python module for physics simulation for games, robotics and machine learning. In <http://pybullet.org>.
  31. McCarthy, Robert, Francisco Roldan Sanchez, Qiang Wang, David Cordova Bulens, Kevin McGuinness, Noel O'Connor, and Stephen J. Redmond. "Solving the Real Robot Challenge using Deep Reinforcement Learning." arXiv preprint arXiv:2109.15233 (2021).
  32. Lillicrap, T. P., Hunt, J. J., Pritzel, A., Heess, N., Erez, T., Tassa, Y., and Wierstra, D. (2015). Continuous control with deep reinforcement learning. arXiv preprint arXiv:1509.02971.
  33. Andrychowicz, M., Wolski, F., Ray, A., Schneider, J., Fong, R., Welinder, P., McGrew, B., Tobin, J., Pieter Abbeel, O. and Zaremba, W., 2017. Hindsight experience replay. *Advances in neural information processing systems*, 30.
  34. Haarnoja, T., Zhou, A., Hartikainen, K., Tucker, G., Ha, S., Tan, J., Kumar, V., Zhu, H., Gupta, A., Abbeel, P. and Levine, S., 2018. Soft actor-critic algorithms and applications. arXiv preprint arXiv:1812.05905.
  35. Schulman, J., Wolski, F., Dhariwal, P., Radford, A. and Klimov, O., 2017. Proximal policy optimization algorithms. arXiv preprint arXiv:1707.06347.
  36. Fujimoto, S., Hoof, H. and Meger, D., 2018, July. Addressing function approximation error in actor-critic methods. In *International conference on machine learning* (pp. 1587-1596). PMLR.
  37. Mnih, V., Kavukcuoglu, K., Silver, D., Graves, A., Antonoglou, I., Wierstra, D. and Riedmiller, M., 2013. Playing atari with deep reinforcement learning. arXiv preprint arXiv:1312.5602.
  38. LeCun, Y., Bengio, Y. and Hinton, G., 2015. Deep learning. *nature*, 521(7553), pp.436-444.
  39. Sutton, R.S. and Barto, A.G., 1999. Reinforcement learning. *Journal of Cognitive Neuroscience*, 11(1), pp.126-134.
  40. Konda, V. and Tsitsiklis, J., 1999. Actor-critic algorithms. *Advances in neural information processing systems*, 12.
  41. Henderson, P., Islam, R., Bachman, P., Pineau, J., Precup, D. and Meger, D., 2018, April. Deep reinforcement learning that matters. In *Proceedings of the AAAI conference on artificial intelligence* (Vol. 32, No. 1).

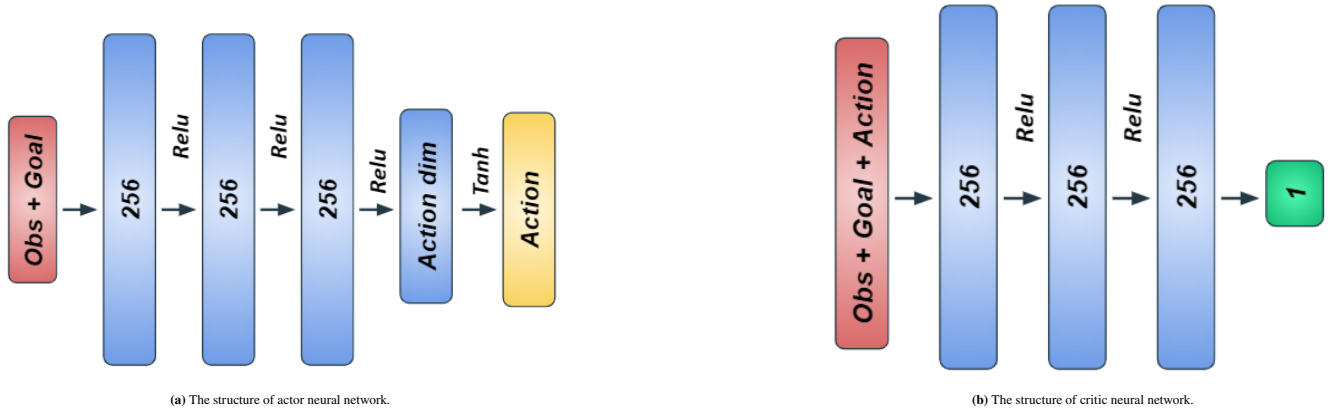


**Figure A1** The neural network structure of the actor and critic. The action output by the actor multiplies the max action ratio before applying it to the environment to make sure it cannot exceed the limits of the action space.



## APPENDIX

### A NEURAL NETWORK

#### A.1 Architecture

The code used in our work are mostly from <https://github.com/TianhongDai/hindsight-experience-replay>, and we have made some edits to adapt it to our environment. The code of *Move Cube on Trajectory* can be found here [https://github.com/RobertMcCarthy97/rrc\\_phase1](https://github.com/RobertMcCarthy97/rrc_phase1), and the code of *Move Cube on Trajectory Pro* can be found here [https://github.com/wq13552463699/rrc\\_pos\\_ori](https://github.com/wq13552463699/rrc_pos_ori). The structures of the actor and critic neural networks is shown in the Figure A1 .

#### A.2 Hyper-parameter

Hyperparameter related to the task/training/testing can be seen in the sub-folder *rrc\_example\_package/her/arguments.py* of the GitHub repositories above.

- *Learning rate of the actor*: 0.001
- *Learning rate of the critic*: 0.001
- *Discount factor*: 0.98
- *Batch size*: 256
- *The average coefficient for soft-update of the target networks*: 0.95
- *Replay buffer size*: 1,000,000
- *HER replay strategy*: future

## B RAW DATA

Ser.	Seed 0		Seed 123		Seed 200	
	Roboch1	Sim	Roboch 6	Sim	Roboch5	Sim
Eva1	-12115	-8288	-15639	-9200	-10120	-8379
Eva2	-15167	-9430	-14262	-12781	-16159	-12284
Eva3	-23378	-8290	-8257	-10560	-21487	-9197
Eva4	-21338	-10045	-11242	-9759	-23810	-7111
Eva5	-25971	-7998	-11947	-8762	-10207	-9745
Eva6	-13497	-8878	-18063	-8536	-12042	-9183
Eva7	-17905	-9567	-13341	-10685	-12958	-9670
Eva8	-22253	-9332	-15494	-10022	-15986	-15520
Eva9	-11608	-7669	-12824	-7113	-18867	-10239
Eva10	-11805	-8351	-21261	-15298	-17593	-8557
Eva11	-10500	-8677	-20369	-9053	-16410	-16587
Eva12	-19996	-9367	-23302	-9123	-18469	-11242
Eva13	-20676	-8585	-18059	-8727	-11228	-13206
Eva14	-12666	-7764	-18087	-8337	-10918	-12380
Eva15	-11413	-9877	-13749	-10143	-14727	-23389
Avg	<b>-16686</b>	<b>-8808</b>	<b>-15726</b>	<b>-9873</b>	<b>-15399</b>	<b>-11779</b>

**Table B1** The evaluated scores of RL agents trained under different seeds on both simulator and real-robot. All RL agents are trained with DR from scratch. We did not run multiple times for each agent on the real robot for saving the source, because agent’s performances are generally poor. This table is the a part of the raw data of Table 3 before averaging.

Ser Nom	Seed 0				Seed 123				Seed 200			
	Rob1	Rob5	Robo6	Sim	Rob1	Rob5	Rob6	Sim	Rob1	Rob5	Rob6	Sim
Eva1	-9970	-11190	-11512	-5635	-8789	-7328	-10030	-6579	-22824	-12436	-11927	-6965
Eva2	-11412	-9017	-11461	-5029	-8086	-10263	-13828	-6650	-12288	-10107	-19633	-7464
Eva3	-10746	-12084	-10900	-5175	-11328	-9908	-8270	-7180	-10859	-9501	-17123	-8839
Eva4	-7572	-15767	-11904	-5570	-9928	-8228	-9110	-6314	-19834	-11469	-15823	-5422
Eva5	-10883	-10430	-13682	-5430	-13106	-8263	-10662	-5746	-13174	-17859	-9643	-7505
Eva6	-7896	-11427	-10371	-5895	-11644	-10245	-6619	-5932	-18568	-14007	-17594	-7324
Eva7	-7942	-14505	-14028	-4977	-6447	-11307	-12355	-6106	-12754	-10631	-11542	-6473
Eva8	-8461	-11135	-13604	-5698	-9180	-7481	-11375	-6551	-21177	-11721	-14255	-6009
Eva9	-6441	-12871	-9460	-4921	-10841	-6781	-7524	-6560	-12986	-11987	-15043	-7716
Eva10	-11466	-11620	-10030	-5702	-4951	-8415	-10385	-6257	-10326	-12408	-17208	-8291
Eva11	-9513	-5192	-15004	-5259	-9020	-8248	-7751	-6055	-18069	-11129	-19162	-7405
Eva12	-11928	-10046	-11051	-6016	-6250	-9530	-11040	-6722	-19168	-19332	-18368	-6590
Eva13	-14798	-11213	-12311	-5027	-8987	-10205	-11442	-7148	-15011	-15671	-15546	-8015
Eva14	-10501	-12419	-16049	-5531	-8834	-9002	-9852	-6101	-23270	-17366	-19554	-6483
Eva15	-9178	-10589	-11256	-5847	-12243	-8691	-16036	-5732	-13678	-11187	-13829	-8657
Avg	<b>-9914</b>	<b>-11300</b>	<b>-12175</b>	<b>-5448</b>	<b>-9309</b>	<b>-8926</b>	<b>-10017</b>	<b>-6376</b>	<b>-16266</b>	<b>-13121</b>	<b>-15750</b>	<b>-7277</b>

**Table B2** Similar as above, but in this table all RL agents are trained from scratch without DR. This table is the raw data of Table 3 and Table 2 before averaging.



Ser.	Seed 0				Seed 123				Seed 200			
	Rob1	Rob5	Robo6	Sim	Rob1	Rob5	Rob6	Sim	Rob1	Rob5	Rob6	Sim
Eva1	-8787	-9647	-7396	-5257	-7579	-6335	-6700	-6461	-8000	-10161	-7614	-5413
Eva2	-11681	-6962	-10088	-6809	-6344	-6729	-7252	-5724	-8219	-9995	-8555	-6481
Eva3	-6013	-8187	-6318	-5442	-7376	-6124	-5388	-7291	-13052	-7443	-6707	-6812
Eva4	-10352	-6727	-4912	-5169	-5364	-8417	-7932	-6066	-12318	-8324	-7532	-7491
Eva5	-8789	-7936	-7370	-6081	-9498	-8711	-6013	-6474	-10980	-7155	-8574	-5620
Eva6	-10460	-11045	-7351	-5908	-8529	-7367	-5514	-5788	-11110	-6375	-7533	-8658
Eva7	-8279	-10296	-11356	-6426	-6393	-4906	-8937	-6458	-7776	-6660	-7679	-5728
Eva8	-10261	-9046	-6375	-6043	-4557	-7492	-7335	-5680	-8995	-9554	-6193	-6664
Eva9	-6371	-11219	-6704	-4671	-7729	-6269	-7673	-6544	-9650	-7126	-7821	-6263
Eva10	-10443	-11136	-11567	-6491	-8103	-9095	-9221	-7921	-10734	-9523	-5636	-6289
Eva11	-6236	-7585	-11795	-5751	-5496	-7470	-5685	-5299	-11455	-7360	-6246	-5608
Eva12	-8060	-6528	-10957	-3804	-6306	-9059	-8037	-5429	-8518	-5751	-9680	-4373
Eva13	-9808	-8811	-8557	-5418	-5114	-6558	-8175	-5993	-7719	-9358	-9330	-5051
Eva14	-10962	-11804	-11804	-7607	-6388	-6056	-6038	-6394	-10331	-7711	-8775	-5891
Eva15	-7681	-7249	-10592	-6500	-7062	-6800	-7225	-6278	-10197	-8043	-6610	-5868
Avg	<b>-8946</b>	<b>-8945</b>	<b>-8876</b>	<b>-5825</b>	<b>-6789</b>	<b>-7159</b>	<b>-7142</b>	<b>-6253</b>	<b>-9937</b>	<b>-8036</b>	<b>-7632</b>	<b>-6147</b>

**Table B3** Similar as above, but in this table all RL agents are trained from scratch without DR and then tuned by DR. This table is a part of the raw data of Table 3 before averaging.

Ser.	ACTOR-CRITIC		ACTOR		COLLECT		SCRATCH		TEACHER	
	Pos(m)	Ori(rad)	Pos(m)	Ori(rad)	Pos(m)	Ori(rad)	Pos(m)	Ori(rad)	Pos(m)	Ori(rad)
Eval1	0.0201	1.3000	0.0698	1.7481	0.0248	1.5535	0.1654	2.5957	0.0215	2.0159
Eval2	0.0253	1.2571	0.0643	1.6544	0.0304	1.6287	0.1143	2.4134	0.0243	2.0639
Eval3	0.0185	1.4060	0.0579	1.7415	0.0301	1.4512	0.1512	2.3510	0.0178	2.1255
Eval4	0.0227	1.3226	0.0797	1.8560	0.0276	1.5742	0.1127	2.5419	0.0304	2.3097
Eval5	0.0221	1.2786	0.0651	1.8221	0.0341	1.4510	0.1208	2.2099	0.0242	2.2001
Eval6	0.0262	1.3984	0.0664	1.7988	0.0271	1.4512	0.1310	2.3118	0.0274	2.3187
Eval7	0.0243	1.2020	0.0691	1.6806	0.0349	1.5679	0.1049	2.4833	0.0204	2.3480
Eval8	0.0198	1.1144	0.0619	1.6527	0.0226	1.3843	0.1732	2.3918	0.0277	2.4137
Eval9	0.0308	1.3189	0.0639	1.6251	0.0297	1.4060	0.1406	2.5777	0.0326	2.2128
Eval10	0.0219	1.2269	0.0611	1.6519	0.0340	1.7080	0.1248	2.6528	0.0264	2.1901
Eval11	0.0225	1.7139	0.0601	1.6495	0.0339	1.4148	0.1215	2.5674	0.0226	2.1884
Eval12	0.0206	1.5068	0.0738	1.8200	0.0320	1.4506	0.1141	2.4648	0.0238	2.2346
Eval13	0.0216	1.3547	0.0694	1.7752	0.0331	1.3885	0.1280	2.4678	0.0200	1.9490
Eval14	0.0255	1.2386	0.0626	1.6965	0.0357	1.3612	0.1348	2.5125	0.0242	2.2067
Eval15	0.0227	1.1980	0.0666	1.7335	0.0287	1.4212	0.1604	2.6438	0.0179	2.2718
Avg	<b>0.0230</b>	<b>1.3225</b>	<b>0.0661</b>	<b>1.7270</b>	<b>0.0306</b>	<b>1.4808</b>	<b>0.1332</b>	<b>2.4790</b>	<b>0.0241</b>	<b>2.2033</b>

**Table B4** The evaluated performance of agent with different KT policies. Where Pos is the deviation between actual and desired position and Ori is that of the orientation. The deviation is calculated by averaging the accumulated reward over 120,000 time-step